Microscopic observation and micromechanical modeling to predict the enhanced mechanical properties of multi-walled carbon nanotubes reinforced crosslinked high density polyethylene

ARTICLE *in* CARBON · FEBRUARY 2014

Impact Factor: 6.2 · DOI: 10.1016/j.carbon.2013.10.020

4 AUTHORS:

Eleftheria Roumeli
ETH Zurich
20 PUBLICATIONS **108** CITATIONS
SEE PROFILE

Eleni Pavlidou
Aristotle University of Thessaloniki
208 PUBLICATIONS **2,702** CITATIONS
SEE PROFILE

Dimitrios N Bikiaris
Aristotle University of Thessaloniki
297 PUBLICATIONS **6,977** CITATIONS
SEE PROFILE

K. Chrissafis
Aristotle University of Thessaloniki
176 PUBLICATIONS **2,516** CITATIONS
SEE PROFILE

CARBON 67 (2014) 475–487

Available at www.sciencedirect.com

ScienceDirect

journal homepage: www.elsevier.com/locate/carbon

Microscopic observation and micromechanical modeling to predict the enhanced mechanical properties of multi-walled carbon nanotubes reinforced crosslinked high density polyethylene

E. Roumeli [a], E. Pavlidou [a], D. Bikiaris [b], K. Chrissafis [a,*]

[a] Solid State Physics Department, School of Physics, Aristotle University of Thessaloniki, Thessaloniki 541424, Greece
[b] Laboratory of Polymer Chemistry and Technology, Department of Chemistry, Aristotle University of Thessaloniki, Thessaloniki 54124, Greece

ARTICLE INFO

Article history:
Received 14 May 2013
Accepted 9 October 2013
Available online 17 October 2013

ABSTRACT

In this work, the significantly improved mechanical performance of crosslinked high density polyethylene reinforced with multi-walled carbon nanotubes (MWCNTs) is examined. The combined results of tensile properties, scanning and transmission electron microscopy (SEM, TEM) and micro-Raman spectroscopy revealed a major turning point of the elastic and deformation behavior of these composites as a consequence of filler content. This experimentally detected behavioral turning point inspired the use of various micromechanical models for the prediction of the composites' elastic behavior. A modern three-phase approach accounting for the matrix, aggregated and finely dispersed filler states adequately describes the experimental data below the turning point, while for higher concentrations, a standard two-phase model is selected to describe the nanocomposites' elastic behavior.

The selectedmodels successfully predicted the exact point of the behavioral transition while highlighting the necessity to use conventional along with modern experimentally-driven methods. Based on the combination of microscopic observations and micro-Raman analysis, it is suggested that the observed and modeled change in the mechanical behavior occurs as a consequence of two competitive mechanisms governing the incorporation of MWCNTs in PEX: a tendency to enhance its mechanical properties by successful load transfer and a drive to form bundles, reducing this positive effect.

1. Introduction

Polyethylene (PE) in all its forms is the most widely used polyolefin with numerous applications based on its attractive features and properties like light weight, low cost, high chemical resistance, low dielectric constant and easy processing techniques. However some important limitations such as low operating temperature narrow the possible uses of PE drastically. Physical or chemical crosslinking provides an effective way of overcoming these drawbacks with relatively easy and low-cost procedures. Either chemically or physically crosslinked high density polyethylene (PEX) extends the use of PE by raising its operating limit at much high temperatures and improving its mechanical properties due to the formation of a 3D structure [1–3]. Since PEX is currently massively produced by the industry for hot and cold water tubing, cables

* *Corresponding author:* Tel./fax: +30 2310998188.
E-mail address: hrisafis@physics.auth.gr (K. Chrissafis).
0008-6223/$ - see front matter
http://dx.doi.org/10.1016/j.carbon.2013.10.020

and wires, heat shrinkable materials and steam resistant food packaging [3], the further enhancement of its properties is of high interest.

Carbon nanotubes (CNTs) have exceptional mechanical, thermal and electric transport properties [4–8] which make them ideal candidates for reinforcing conventional materials in order to produce superior composites for a wide range of applications. During the past decades the polymer research community, both academic and industrial, has devoted a lot of work on the synthesis and study of CNTs-polymer composites seeking to reach the excellent performance of CNTs [9–13]. CNTs-reinforced polymers have already shown exciting results with enhanced important polymer properties at exceedingly low filler concentrations [14]. Among other desirable properties that CNT-based nanocomposites are intending to achieve, are the outstanding strength and stiffness of CNTs. It has been suggested that an effective load transfer between the matrix and the filler may be the key to superior elastic modulus and strength of the composite [15,16] and therefore its thorough investigation is of great importance. A successful load transfer between lies in a combination of homogeneous dispersion and interaction of CNTs with the surrounding matrix [17]. Considering the nanotubes' agglomeration due to the electrostatic interaction and van der Waals forces, CNTs dispersion can be a real challenge.

An equally challenging task is the theoretical prediction of the behavior of such nanocomposites. There have been many efforts to develop micromechanical models to predict composites' behavior but they are usually tested in simulated data [18,19]. Very few articles can be found in literature applying micromechanical models in polymer nanocomposite systems due to their rather peculiar behavior, which is greatly dependent on the preparation and further processing methods, making predictions of their properties extremely challenging with conventional approaches. In this work, various micromechanical models have been tested and compared with experimental results, all the way from classical geometrical bounds approaches [20] to the two-phase models with percolating network concept embedded [21] and from mean field approximations [22,23] to more recently proposed three-phase models [24]. The models that were selected to be tested are critically presented and the proposed combination of models is justified by experimental findings while their foundation is considered valid for the studied nanocomposites. Moreover, the proposed combination of models is extremely interesting as it reflects the necessity to rely not only on classic original concepts, like that of Takayanagi [25], but also on modern attempts which embrace experimental evidence like that proposed by Loos et al. [24].

The aim of the present work is to report the mechanical reinforcement of crosslinked high density polyethylene nanocomposites containing MWCNTs prepared by melt mixing and examine the superior mechanical performance, elastic and fracture behavior of the composites, suggest a successful model to predict the elastic modulus of this system and finally study the load transfer between the matrix and the nanofiller during tension.

2. Experimental section

2.1. Materials

High density polyethylene grafted with vinyl trimethoxysilane (g-HDPE) was kindly supplied by Sioplas S.A. with a Mn of 28,000, Mw 120,200 and intrinsic viscosity 1.54 dl/g. A catalyst masterbatch containing the same HDPE along with dibutyltin dilaurate (DBTDL), internal lubricants, stabilizers and various antioxidants was also supplied by Sioplas. The catalyst batch can accelerate the hydrolysis reaction of the grafted silyl groups with water to form silanols, the condensation of silanols to form siloxane bonds or both. The hydrolysis and condensation reactions are shown in Figs. 1 and 2.

Purified multi-walled carbon nanotubes were purchased from Chengdu Organic Chemicals Co. Ltd. The inner and outer diameters of MWCNTs were less than 2–5 and 8 nm, respectively and they have 2.1 g/cm^3 density.

2.2. Nanocomposites preparation

Prior to melt mixing, solid state ball milling was employed in order to achieve a fine dispersion of the MWCNTs in the polymer matrix. Mixtures of 95 parts of g-HDPE, 5 parts of catalyst masterbatch and 0.5, 1, 3 and 5 wt% MWCNTs were solid-state mixed for 6 h in a Retsch centrifugal ball mill (model S 100). A cylindrical stainless steel jar of 50 ml with 6 steel balls of 10 mm in diameter were used and a rotation speed of 500 rpm was applied. Each mixture after ball milling were melt-mixed in a Haake-Buchler Rheomixer (model 600) with roller blades and a mixing head with a volumetric capacity of 69 cm^3. During the mixing period the melt temperature and torque were continuously recorded. For this case a 10 min mixing at 200 °C with a torque speed of 60 rpm were used. The prepared samples were immediately hot pressed using an Otto Weber, Type PW 30 hydraulic press connected with an Omron E5AX Temperature Controller, at a temperature of 180 ± 5 °C, in order to prepare films of 10–30 and 350–450 μm thickness appropriate for each type of measurement. The films were rapidly cooled by immersion in water at 25 °C. Finally, all prepared films were exposed to a hot bath (90 °C water for 24 h) to complete the crosslinking process in the bulk of the polymer as shown in Figs. 1 and 2.

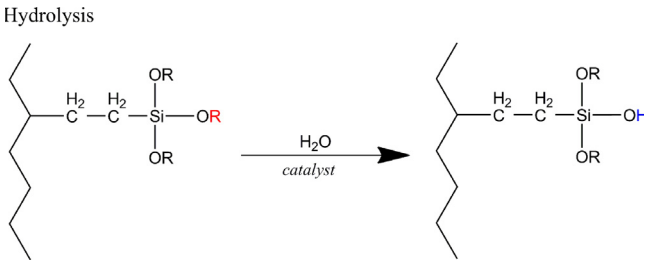

Fig. 1 – Hydrolysis reactions of HDPE grafted trimethoxysilane. (A colour version of this figure can be viewed online.)

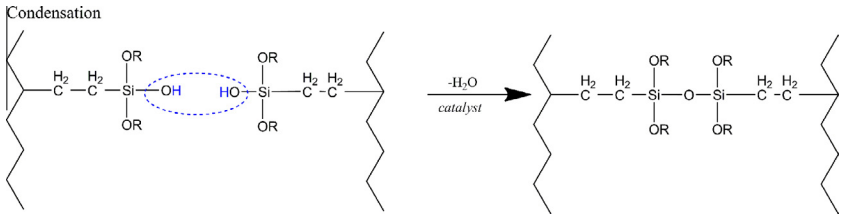

Fig. 2 – Condensation reactions taking place during crosslinking of HDPE. (A colour version of this figure can be viewed online.)

2.3. Methods

2.3.1. Mechanical properties

Mechanical properties testings were performed on an Instron 3344 dynamometer, in accordance with ASTM D638 using a cross-head speed of 50 mm/min. Sheets of about 350–450 μm thickness were used, prepared as described previously. In order to measure the mechanical properties from these sheets, dumb-bell-shaped tensile test specimens (central portions 5 × 0.5 mm thick, 22 mm gauge length) were cut in a Wallace cutting press. At least five measurements were conducted for each sample, and the results were averaged to obtain a mean value. The values of Young's modulus, tensile strength at yield and at break point and elongation at break were determined.

2.3.2. Scanning electron microscopy (SEM)

The dispersion of MWCNTs and the morphology of the failure surfaces of all nanocomposites after tensile testing were examined in a SEM system (JEOL JSM 840A-Oxford ISIS 300 microscope). The specimens were carbon coated in order to provide good conductivity of the electron beam. Operating conditions were: accelerating voltage 20 kV, probe current 45 nA, and counting time 60 s.

2.3.3. Transmission electron microscopy (TEM)

The dispersion and morphology of MWCNTs was also examined by transmission electron microscopy (TEM) images that were taken from on ultra-thin film samples of the various nanocomposites cut by an ultra-microtome. The thin sections were deposited on copper grids. TEM micrographs were obtained using a JEOL 120 CX microscope operating at 120 kV.

2.3.4. micro-Raman spectroscopy

Raman spectroscopy measurements were performed using a micro-Raman spectrometer (LabRAM HR; Horriba Jobin Yvon Ltd, UK, with LABSPACE software) with a CCD camera detector. An excitation wavelength at 632.8 nm was provided by a He–Ne laser. The spectral range was 3500–700 cm^{-1} with confocal hole at 1000 μm, slit at 100 μm, grating at 1800, microscope objective ×50 while exposure time and accumulation for measuring were 5 s and two times, respectively.

3. Results and discussion

3.1. Morphology of MWCNTs and nanocomposites

SEM and TEM micrographs of the MWCNTs used in this work are shown in Fig. 3. From these images it can be seen that the nanotubes have a several microns length and their thickness varies from 5 to 15 nm. Some nanotubes are entangled and some are helically shaped which may assist a better embedding in the matrix than the straight nanotubes.

In Fig. 4 TEM micrographs of all nanocomposites with MWCNTs are presented. As revealed from these micrographs, at low filler concentration (up to 1 wt%), the nanotubes are well dispersed in the matrix and they do not form large aggregates. As concentration increases (Fig. 4e–g), the intrinsic van der Waals attractions between the individual nanotubes lead to the formation of more and considerably larger aggregates. However, an overall satisfying dispersion of the formed aggregated nanotubes can be seen even in the samples with the highest filler loading. The formation of a continuous network of MWCNTs which would prove the filler percolating theory was not observed in any case from the microscopy images.

The absence of chemical interactions through bonds between the matrix and the fillers as evidenced by FTIR (Supplementary material) and Raman spectroscopy measurements (presented in a following section) reveals that the weaker van der Waals attractions between MWCNTs cause their observed agglomeration, while the shear force from melt-mixing is leading to randomly arrayed nanotubes. The overall fine dispersion of MWCNTs in the matrix for the nanocomposites with lower filler content, which is essential for making reinforced polymer composites with superior mechanical properties, proves that the shear mixing forces overcome the intrinsic van der Waals attractions of MWCNTs. Yet when MWCNTs concentration exceeds a certain limit (1 wt% as evidenced by TEM images), the shear mixing forces are not strong enough to prevent MWCNTs agglomeration even though they cause a good dispersion of the formed aggregates.

3.2. Mechanical properties of the nanocomposites

The main goal of the present work was to reinforce PEX with MWCNTs and prepare nanocomposites with superior

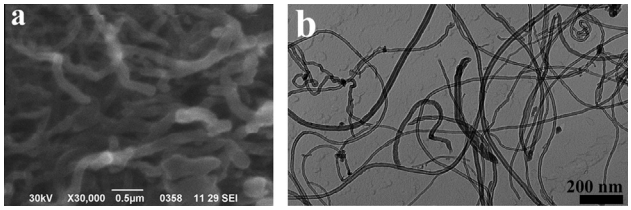

Fig. 3 – (a) SEM and (b) TEM micrographs of the used MWCNTs.

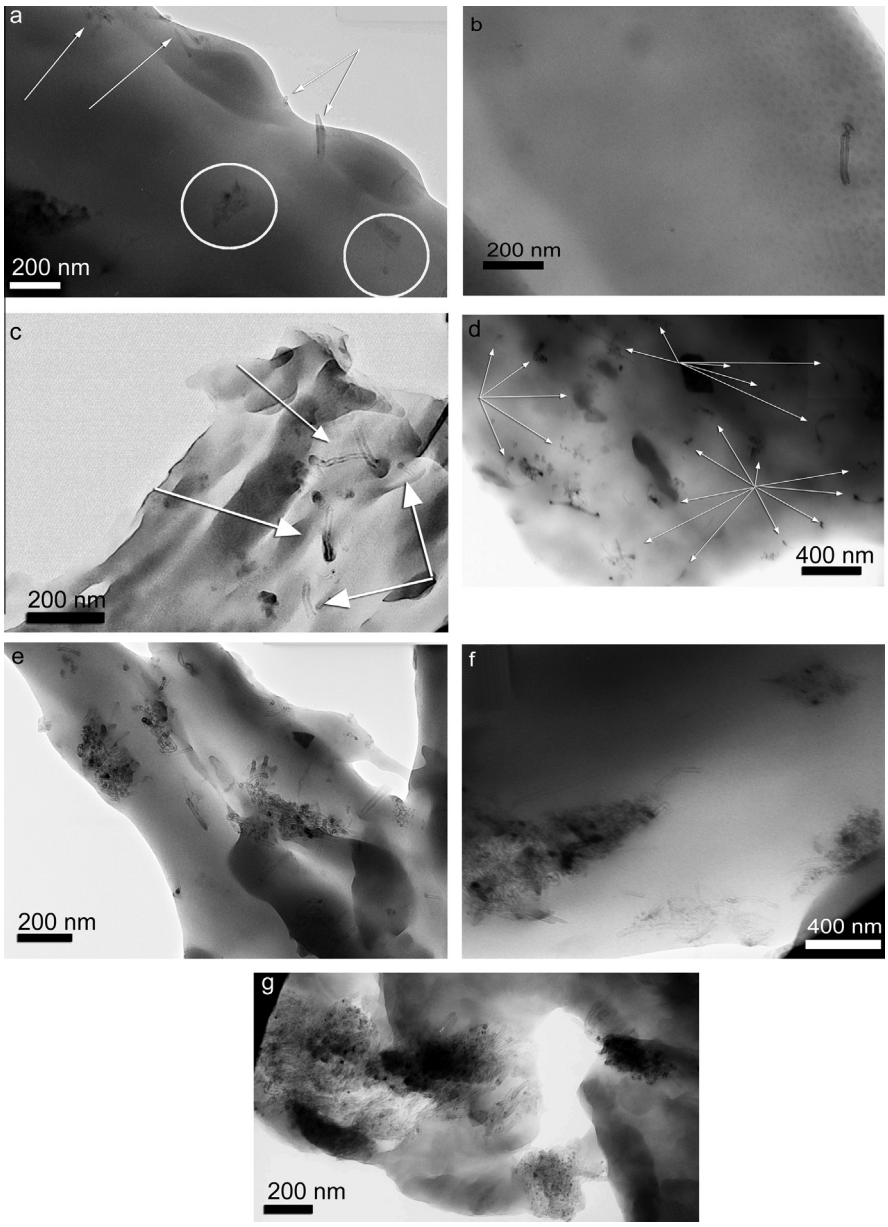

Fig. 4 – TEM micrographs of PEX nanocomposite containing (a and b) 0.5%, (c and d) 1, (e and f) 3 and (g) 5 wt% MWCNTs.

Table 1 – Mechanical properties of all studied materials.

MWCNTs (% wt)	Young's modulus (MPa)	Strength at yield (MPa)	Strength at break (MPa)	Elongation at break (%)
0	675 ± 35	19.8 ± 0.7	22.0 ± 2.0	420 ± 21
0.5	776 ± 11	23.2 ± 0.4	26.8 ± 1.1	494 ± 20
1	742 ± 15	23.2 ± 0.4	28.9 ± 1.4	456 ± 31
3	736 ± 15	23.1 ± 1.1	22.0 ± 1.1	338 ± 41
5	985 ± 40	29.6 ± 1.7	21.8 ± 1.3	150 ± 10

mechanical properties. The results of the tensile tests are presented in Table 1 and they reveal a significant enhancement of all the mechanical properties of PEX when MWCNTs are incorporated in the matrix. The addition of 0.5% MWCNTs leads to a 100 MPa enhancement of Young's modulus while a further increase of MWCNTs content leads to elastic modulus values higher than neat PEX but somewhat lower than the nanocomposite with 0.5% MWCNTs. However, the nanocomposite with 5% MWCNTs has the highest elastic modulus (985 MPa) which is 310 MPa higher than the neat

polymer's. Tensile strength at yield point seems to follow the same trend; in the case of 0.5% MWCNTs the strength at yield is 3.4 MPa higher than that of neat PEX. For the nanocomposites with 1–3% MWCNTs, the strength at yield remains almost the same as for the nanocomposite with 0.5% MWCNTs, while for the nanocomposite with 5% MWCNTs the strength at yield is considerably higher (9.8 MPa higher than in neat PEX).

A somewhat different behavior was found for the strength and elongation at break of the nanocomposites. It seems that the small amounts of MWCNTs (up to 1 wt%) lead to a notable increase of 6.9 MPa for the strength at break while a higher MWCNTs concentration causes a reduction of the ultimate strength, which reaches the same level as neat PEX. The elongation at break of the nanocomposites presents a similar trend to the ultimate stress values. Up to 1% MWCNTs the elongation at break values are higher than in neat PEX, while for higher filler content they are drastically reduced. Similar behavior has also been reported in literature for other types of polyethylene-MWCNTs nanocomposites [26–28]. The elongation at break decrease for the nanocomposites with higher filler content is probably caused by the stress concentration effect of MWCNTs [29]. The increased filler content leads to higher probability of filler aggregation, which results in the formation of regions of stress concentrations that require less energy to propagate cracks. During tensile deformation, the stress cannot be transferred efficiently near these areas, resulting in failure. Furthermore the much higher rigidity of MWCNTs means that the elongation at break is mainly due to the matrix and therefore decreasing its content would result in the decrease the elongation to break [29].

By studying the stress-strain curves of the composites, another interesting behavior was observed. The neat polymer has a ductile fracture behavior as the stress at break is higher than the stress at yield and a large plastic deformation is the predominant mechanism of failure. The same ductile behavior was observed for the nanocomposites with low filler content (up to 1% wt). In these composites the plastic deformation area is even larger than the neat PEX which means that they are tougher than the neat polymer. The composites with higher filler content (3–5 wt%) present a brittle fracture behavior as the stress at yield is higher than the stress at break and also the plastic deformation upon failure is significantly lower than in the other composites. Thus, a change in the deformation mechanism is observed as a consequence of filler content: low filler content (up to 1 wt%) retains the ductile behavior of the original polymer while higher loadings result in a more brittle performance.

The observed behavior of the studied materials suggests that the presence of MWCNTs in PEX leads to an enhancement of its elastic modulus and ultimate stress (at yield and at break points) while their bundles and possible local poor dispersion tend to reduce this effect. It has been proved that the aggregates of nanotubes effectively reduce the aspect ratio of the reinforcement causing a reduction of the elastic properties of the composite [30]. In fact, the properties of large diameter MWCNTs bundles are dominated by shear slippage of individual nanotubes within the bundle. This inter-tube slippage within bundles lowers to a great extent their intrinsic mechanical properties and may partially explain the decrease in the modulus of a polymer composite at high volume fraction of MWCNTs.

Therefore, it is proposed that two competitive mechanisms act upon the incorporation of MWCNTs in PEX: below the turning point of 1 wt%, the shear mixing forces overcome the van der Waals attractions between the MWCNTs, leading to their fine dispersion in PEX and therefore, through the successful load transfer between the filler and the matrix, the composites have greatly enhanced mechanical properties. However, when filler concentration exceeds the limit of 1 wt%, the intrinsic nanotube attractions causing the formation of agglomerates are comparable to the shear forces thus, reducing the positive effect on the mechanical properties. Evidence of the existence of both these mechanisms can be found from the Raman measurements which are thoroughly discussed in the following section and support the successful load transfer and from microscopy observations which revealed the effects of both mechanisms. The behavioral turning point highlights the concentration above which, the molecular attractions between nanotubes become so important that they can be considered comparable to the shear forces during mixing and therefore, they reduce the enhancement of all mechanical properties.

3.3. *Mechanical properties modeling*

The significantly higher elastic modulus of PEX nanocomposites has led us to try to investigate and model the elastic behavior of these materials in order to be able to make predictions for other MWCNTs concentrations. The successful prediction of a composite's mechanical properties remains a challenging topic for the scientific community and to date various micromechanical models have been developed and used. Depending on the matrix, type of filler, physical dimensions of the filler, filler–filler and filler–matrix interactions, etc. more or less the majority of the suggested approaches have successfully or not been tested. In this work we have selected and tested some basic and fundamental methods along with some recently proposed and rather promising ones in order to compare their predictions with our experimental data and evaluate the elastic behavior of the prepared composites.

The first two models are the parallel and series geometrical models that yield the Voigt or Reuss average elastic modulus, respectively [20]. In these two models, the main hypothesis is that the composite consists of two separate, piled-up phases with geometries as shown in Fig. 5a and b.

In the Voigt model the isostrain condition is assumed and therefore the elastic modulus can be calculated from the following equation

$$E_c = E_f V_f + E_m V_m \quad (1)$$

where E corresponds to the elastic modulus and V to the volume fraction and the subscripts c, f and m correspond to composite, filler and matrix, respectively. In that model, the two phases experience the same strain, whereas, the stress is additive.

In the case of the Reuss model, the isostress condition is applied yielding the following equation

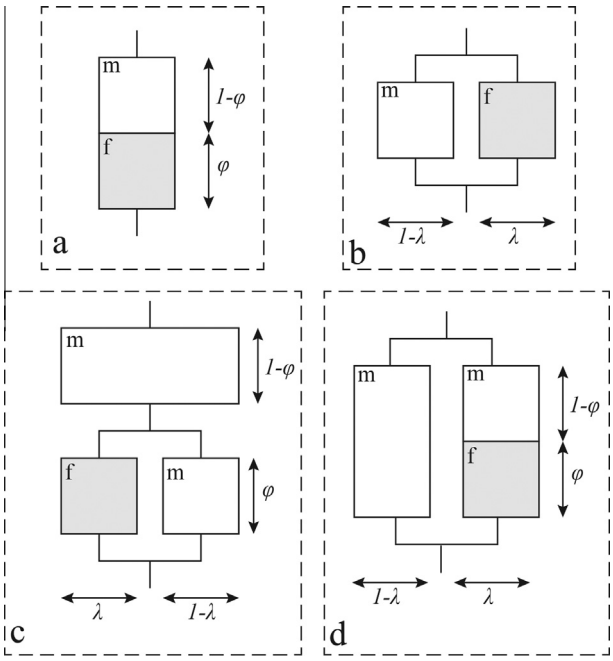

Fig. 5 – Models used in the micromechanical equations: (a) series, (b) parallel, (c) Takayanagi I (series-parallel) and (d) Takayanagi II (parallel-series).

$$\frac{1}{E_c}=\frac{V_f}{E_f}+\frac{V_m}{E_m} \tag{2}$$

In that model, the main assumption is that the composite's phases withstand the same external load and the strain is considered additive.

These initial attempts to model the elastic modulus of composites have been the basis of the significant work of Takayanagi et al. [25] who introduced a combination of series-parallel and parallel-series models (shown in Fig. 5c and d) in order to explain the viscoelastic behavior of a polymer blend system comprised of two components and relate it to the corresponding properties of the individual components.

His efforts on developing appropriate models to account for the mechanical coupling of a two-phase system yielded the following expression for the calculation of elastic modulus using the series-parallel configuration:

$$\frac{1}{E_c}=\frac{\phi}{\lambda E_f+(1-\lambda)E_m}+\frac{1-\phi}{E_m} \tag{3}$$

while for the parallel-series configuration he proposed the following equation:

$$E_c=\lambda\left(\frac{\phi}{E_f}+\frac{1-\phi}{E_m}\right)^{-1}+(1-\lambda)E_m \tag{4}$$

In the Takayanagi models, the assumption of a two-phase system gives a direct uniaxial representation of the presumed mechanical coupling through adequate serial or parallel connections only two adjustable parameters. These parameters, λ and φ, are related to the degree of series-parallel coupling and their product represents the volume fraction of the filler phase in the case of the studied composites.

Using the Takayanagi II model Ouali et al. [21] included the experimentally-suggested percolating filler concept and that model has been one of the most frequently used in polymer composites [31–35] as they often present a percolating behavior. The roots of percolation theory date back to World War II [36] and it is based on the assumption that chemical bonds are formed randomly between the neighboring particles which form clusters. Ouali's model takes into consideration the filler–filler interactions that lead to the percolation concept and is very well adapted to describing a percolating network of micro or nano-fillers in polymer matrices. The Ouali model describes the elastic modulus of the composite based on the elastic moduli of each component, the volume fraction of the filler and the volume fraction of the percolating phase (ψ). The volume of the percolating phase, for filler concentrations higher than the percolation threshold (V_c), can be calculated from a classic power law expression [37]:

$$\psi=\begin{cases}0, & V_f<V_c\\ V_f\left(\frac{V_f-V_c}{1-V_c}\right)^b, & V_f\geq V_c\end{cases} \tag{5}$$

in which the percolation exponent b can be 0.4 for a 3-D percolating system [32].

The percolation threshold, V_c, depends on the filler aspect ratio (r) and based on the excluded volume concept [38–40] a reliable estimation can be made using:

$$V_c=\frac{0.7}{r} \tag{6}$$

The modulus of the composite for the series-parallel model can then be derived from the following:

$$E_c=\frac{(1-2\psi+\psi V_f)E_mE_f+(1-V_f)\psi E_f^2}{(1-V_f)E_f+(V_f-\psi)E_m} \tag{7}$$

Another approach that was employed in the present work is the mean-field approximation which is well illustrated by the Halpin–Tsai model [22,23] and is often used to predict the behavior of composites containing randomly oriented fibers [18,33,41,42]. However, it takes into account the reinforcement effect due to the presence of rigid inclusions in a soft matrix, without considering filler–filler or filler–matrix interactions. It assumes that such materials can be viewed as a group layers containing unidirectional plies oriented at various angles to give a quasi-isotropic composite. The mechanical properties of each ply are derived from the micro-mechanic equations of Halpin–Tsai. One of the main interests of this approach is that it takes into account the anisotropy of the mechanical properties of the filler particle. According to that method, the composite's modulus can be expressed through

$$E_c=E_m\left(\frac{1+\xi\eta V_f}{1-\eta V_f}\right) \tag{8}$$

In which $\xi=2r$ and η can be calculated from the following:

$$\eta=\frac{\frac{E_f}{E_m}-1}{\frac{E_f}{E_m}+\xi} \tag{9}$$

A more modern approach was recently suggested by Loos et al. [24,43] which undertakes the Ouali-modified Takayanagi models as well as the original series and parallel models was also tested in this work. This approach uses instead of two, a three-phase system and suggests that it is comprised of a

polymer matrix, a dispersed nanofiller phase and a percolating filler phase. For simplicity, they considered that all three constituents exhibit a linear elastic behavior and are isotropic. This crucial modification leads to four modified models (modified Reuss, modified Voigt and modified Takayanagi I and II), in which the moduli of each phase are noted with the corresponding superscript *agg* for the aggregated-percolating filler phase and *dis* for the disentangled filler phase. The well-dispersed MWCNTs encompass all non-entangled units, while agglomerated MWCNTs consist of the percolated network (at overall concentration in the system exceeding the threshold value) and all other entangled nanotubes present in the system. The Loos models do not account for nanotube/matrix debonding, slippage at the interface matrix/nanotube, or any voids or cracks present in the system. Their models account for the different mechanical properties of the agglomerated nanotubes from the ones of the well-dispersed nanotubes.

The volume fraction of each component needs to be calculated and therefore, Loos et al. have suggested the use of the f-switching function [18] similar but not the same as Eq. (5), to emulate the percolation behavior above the percolation threshold:

$$f_{(V_f)} = \begin{cases} 0, & V_f < V_c \\ 1 - e^{-A\left(\frac{V_f}{V_c}-1\right)^{0.474}}, & V_f \geq V_c \end{cases} \quad (10)$$

In Eq. (10), the parameter A is an adjustable parameter which modulates the width of the transition. Below the percolation threshold, the filler volume fraction is considered to be entirely due to the dispersed nanotubes, while for concentrations above V_c, the percolating phase volume can be calculated by $V_f^{agg} = fv_f$ and the dispersed phase from $V_f^{dis} = (1-f)v_f$. Using these values for each composite, the elastic modulus can be calculated for the modified parallel model based on Eq. (1), which still corresponds to the upper bound of E_c but now takes the following form:

$$E_c = V_f^{agg}E_f^{agg} + V_f^{dis}E_f^{dis} + \left(1 - V_f^{agg} - V_f^{dis}\right)E_m \quad (11)$$

while for the case of the modified series model which is the low E_c bound and is based on Eq. (2), the composite's modulus can be expressed as:

$$E_c = \frac{E_f^{agg}E_f^{dis}E_m}{V_f^{agg}E_f^{dis}E_m + V_f^{dis}E_f^{agg}E_m + \left(1 - V_f^{agg} - V_f^{dis}\right)E_f^{agg}E_f^{dis}} \quad (12)$$

Eqs. (11) and (12) are reduced to 1 and 2 for filler content below V_c.

The modified Takayanagi model I based on the Ouali percolating concept (Eq. (7)) can be written in the following form:

$$E_c = \frac{(1-V_f)E_mE_f^{agg} + (V_f - \psi)E_f^{dis}E_f^{agg}}{(1-V_f)\psi E_m + \psi(V_f-\psi)E_f^{dis} + (1-\psi)^2E_f^{agg}} \quad (13)$$

while the Takayanagi model II can be expressed as:

$$E_c = \frac{\psi(1-V_f)E_f^{dis}E_f^{agg} + \psi(V_f-\psi)E_mE_f^{agg} + (1-\psi)^2E_mE_f^{dis}}{(1-V_f)E_f^{dis} + (V_f-\psi)E_m} \quad (14)$$

The above models were applied in the experimental values of the elastic modulus in order to evaluate which can be applied in the particular composites and will yield more reliable predictions. The results from the series, parallel and Takayanagi I and II models are presented in Fig. 6a and they reveal that the experimentally determined values are within the boundaries set by the Voigt and Reuss models, while the Takayanagi I and II expressions are peaking in a turning point close to the predicted percolation threshold ($V_c = 0.00175$) and follow the same decreasing trend for 0.5–2.5 MWCNTs wt% and increasing for concentrations higher than 2.5 wt%. From these results, for concentrations higher than 1 wt% the Takayanagi I model seems to fit better the experimental data, while the Takayanagi II presents slightly higher deviations. The composites with filler content below 1 wt% cannot adequately be described by these models.

The results of the Ouali-modified Takayanagi and Halpin-Tsai micromechanical models are presented in Fig. 6b. It can clearly be seen that the mean filed approximation cannot describe the experimental results (it overpredicts the elastic modulus and ignores filler–filler and matrix–filler interactions) whereas the Ouali method suggests an exponential increase of the elastic modulus for filler content above the percolation limit which also does not fit the data. Even though the percolation concept has been successfully applied in many cases, the present study reveals that in its classical form suggested by Ouali, it cannot adequately describe the complex behavior of PEX composites, probably because a percolating network in the sense of a continuous network of MWCNTs was not formed in them. The absence of such a percolating network is also supported by the TEM images (Fig. 4) were the MWCNTs bundles are distinguished and do not form a continuous network.

In Fig. 6c the modified Reuss and Voigt models based on Eqs. (11) and (12) are compared to the experimental data. These models have been modified to include the percolation concept (introduced in the switch function, f) and the different behavior of aggregated and disentangled MWCNTs and therefore, the completely different shape of the Voigt model is due to these modifications. Even in their modified forms, these models can only be used to predict the lower and upper bounds of the composites' modulus. The three phase series model, again gives a lower bound for the composite modulus considering that all three phases experience the same stress and the strain is additive. The three phase parallel model, based on the assumption that all three phases can deform to the same extent upon the application of stress, renders an upper bound to the composite modulus.

In Fig. 6d the modified Takayanagi I and II models based on Eqs. (13) and (14) are plotted and compared to the experimental data, revealing that for lower MWCNTs concentrations (up to 1 wt%) the modified Takayanagi I model yields a better fitting than any other model. However for higher filler content, the modified models can no longer be applied. The modified Takayanagi II model cannot be used in any filler concentration as it results in a worse fitting.

In some studies where the formed filler percolating network has been found to improve the composite's mechanical properties and the Takayanagi II with the percolation concept have been successfully applied to experimental data, the fillers were found to be linked by strong hydrogen bonds [44]. However, in the case of MWCNTs which form a geometrical

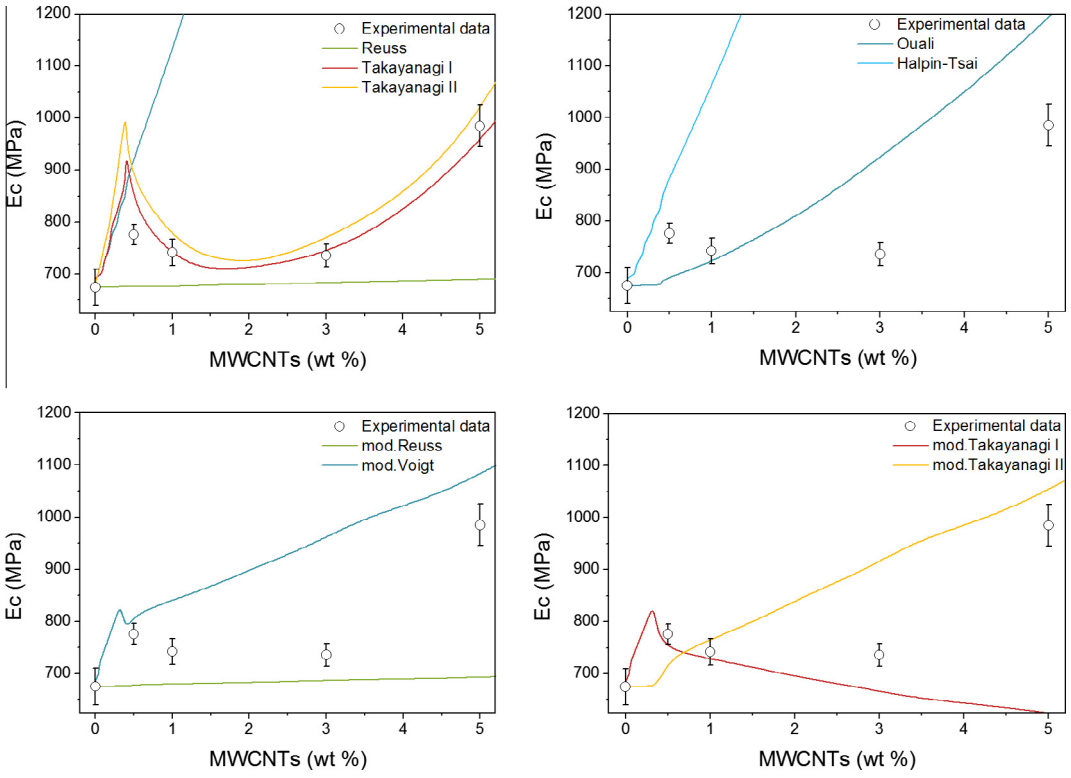

Fig. 6 – Results of all micromechanical models in comparison with the experimental data. (a) The classic models: Reuss, Voigt, Takayanagi I and II, (b) the modified by Ouali et al. Takayanagi I model and Halpin-Tsai model, (c) the modified by Loos et al. Reuss and Voigt models, (d) the modified by Loos et al. Takayanagi I and II models. (A colour version of this figure can be viewed online.)

percolating network without strong hydrogen bonds, the network formation can be detrimental to the system mechanical properties. Such behavior have been reported to be better described using the Takayanagi I model with the percolation concept [43]. From the application of Takayanagi I modified model in our experimental data, it can be confirmed that its use is justified for concentrations below the point where inter-tube interactions become comparable to the shear mixing forces.

In conclusion, a behavioral turning point at 1 wt% MWCNTs was pointed out by the micromechanical modeling analysis (presented in Fig. 7). The nanocomposites with MWCNTs content below 1 wt% can more adequately be described by the modified by Loos et al. Takayanagi I model, while for higher concentrations the un-modified Takayanagi I model yields the best fitting quality. Therefore, the elastic modulus of the prepared composites can be described though the following expression:

$$E_c = \begin{cases} \frac{(1-V_f)E_m E_f^{agg} + V_f E_f^{dis} E_f^{agg}}{E_f^{agg}}, & 0 < V_f < V_c \\ \frac{(1-V_f)E_m E_f^{agg} + (V_f-\psi)E_f^{dis} E_f^{agg}}{(1-V_f)\psi E_m + \psi(V_f-\psi)E_f^{dis} + (1-\psi)^2 E_f^{agg}}, & V_c \le V_f \le \text{turning point} \\ \frac{\lambda E_f E_m + (1-\lambda)E_m^2}{\lambda(1-\phi)E_f + (1-\lambda+\lambda\phi)E_m}, & V_f > \text{turning point} \end{cases} \quad (15)$$

For the composites with filler content below the turning point, which is above the percolation threshold whatsoever, the three-phase approach based on Takayanagi I model can be used to describe the experimental data as in these composites, MWCNTs exist mainly in the dispersed phase even though the formation of a few aggregations could not be avoided as evidenced by TEM observations. Therefore, a three-phase model accounting for a dispersed and an agglomerated phase is a plausible selection.

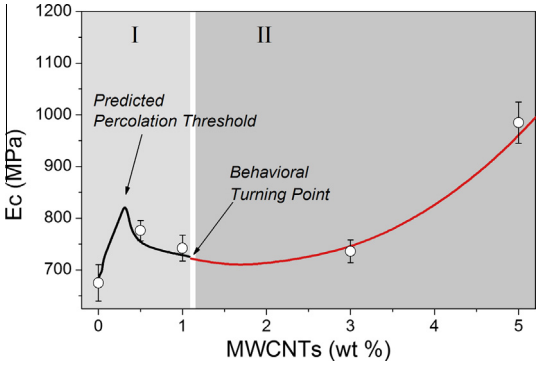

Fig. 7 – Application of the modified Takayanagi I model for filler concentrations below 1 wt% and unmodified Takayanagi I model for higher filler concentrations for the prediction of elastic modulus of PEX/MWCNTs nanocomposites. (A colour version of this figure can be viewed online.)

For the composites with MWCNTs content above the turning point of 1 wt%, the intrinsic attractions between the nanotubes become comparable to the shear mixing forces and the

formed aggregations are becoming more and larger, leading to a less pronounce enhancement of the elastic modulus for concentrations between 1 and 3 wt%. Therefore, the concept of a third phase consisting of a dispersed MWCNTs amount can no longer be valid. Thus, the fitting results which revealed that un-modified Takayanagi I model is more suitable for these concentrations are reasonable, as these systems need to be considered as two-phase systems. The failure of the percolating models of Ouali and modified Takayanagi for composites with MWCNTs content above 1 wt% can also be supported though the TEM observations which revealed MWCNTs aggregations but not in any case the formation of a continuous network between them.

The proposed combination of conventional and modern models from this study, is an exceptional way to demonstrate the necessity to adjust new experimental findings, such as the CNTs' different behavior in the dispersed and aggregated phase, on reliable original concepts in order to predict real polymer nanocomposite systems' behavior, which can otherwise not be described from a solely conventional methods point of view.

Thus, the previously discussed transition (from ductile to brittle) of the deformation mechanism was detected in the same turning point in which the micromechanical elastic properties models change. The combination of these findings confirms the proposed competitive mechanisms that act upon MWCNTs incorporation in the polymer matrix.

3.4. *Examination of failure surfaces and behavior of PEX and nanocomposites*

Following the thorough examination of the elastic behavior of the nanocomposites, an equally deep comprehensive study of the fracture behavior was performed. The SEM investigation of the failure surfaces of all nanocomposites after tensile testing revealed some very interesting results and representative images are shown in Figs. 8–12. In Fig. 8 the neat polymer's failure surface can be seen. Dasari et al. have recently shown microscopy images which prove that during uniaxial tensile deformation of high density polyethylene (HDPE), the transition from the initial spherulitic structure by plastic deformation to the final fibrillar structure involves the destruction of the lamellae, alignment and orientation of structure by longitudinal sliding motion of micro-fibrils [45,46]. Tensile deformation processes in HDPE involve stretching of fibrils resulting in the formation of surface openings. A similar fibrillar structure upon plastic deformation and failure was observed in the present case of crosslinked polyethylene as well (Fig. 8). From the closer detail view the failure surfaces after deformation of PEX can be clearly seen.

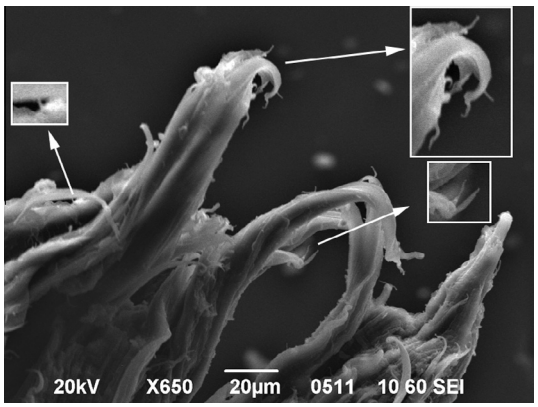

Fig. 9 – SEM image of the fracture surface after tensile testing of PEX nanocomposite containing 5% MWCNTs. Broken hanging MWCNTs and bridged MWCNTs can be seen.

In Figs. 9–12 some typical overviews of the failure surfaces of the nanocomposites are presented. The nanotubes are pointed out in most of these images and their several microns length can clearly be seen. The characteristic fibrillar structure of PEX at failure was also observed in all its nanocomposites. Upon failure, most of the MWCNTs were broken while a few were pulled out of the matrix as shown in Figs. 9–12. Broken nanotubes can clearly be seen in Figs. 9 and 10 and in the inset detail images. Many of the nanotubes had one or both ends still strongly embedded in the matrix. As revealed by Coleman et al. polymeric matrices can form coatings covering the nanotubes protruding from composite fracture surfaces [47]. Therefore, the higher than expected tube widths that can be observed in some of the images may be polyethylene-covered nanotubes.

A representative plane view fracture surface of the nanocomposites is shown in Fig. 11 and it consists of MWCNTs (possibly covered by polyethylene) evenly distributed on the surface. From the morphology of the nanotube network it looks as if the tube bundles have been pulled out of the matrix during the deformation and fracture of the composites.

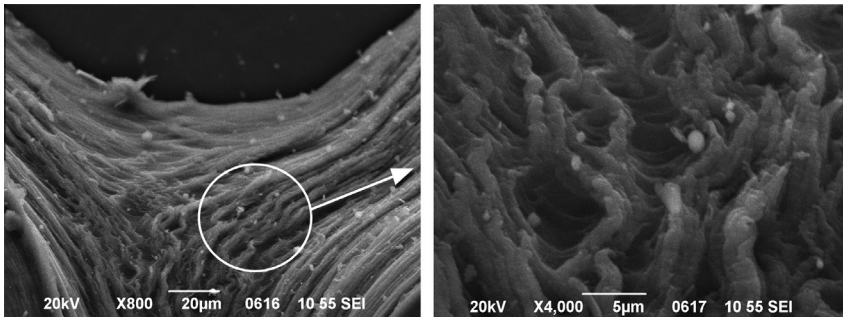

Fig. 8 – SEM observation of the fracture surface after tensile testing of neat PEX (left) and detail image (right).

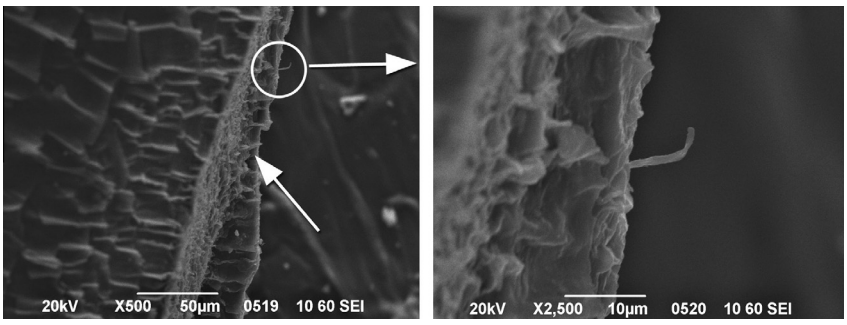

Fig. 10 – SEM image of the fracture surface after tensile testing of PEX nanocomposite containing 3% MWCNTs (left) and detail (right). The stretched hanging MWCNTs can be seen from both images.

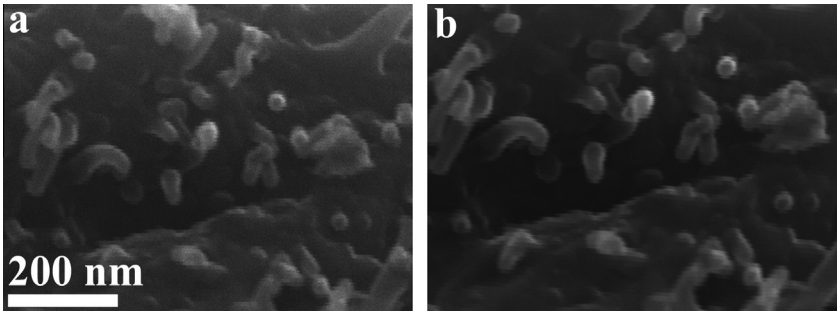

Fig. 11 – SEM image of the fracture surface after tensile testing of PEX nanocomposite containing 3% MWCNTs.

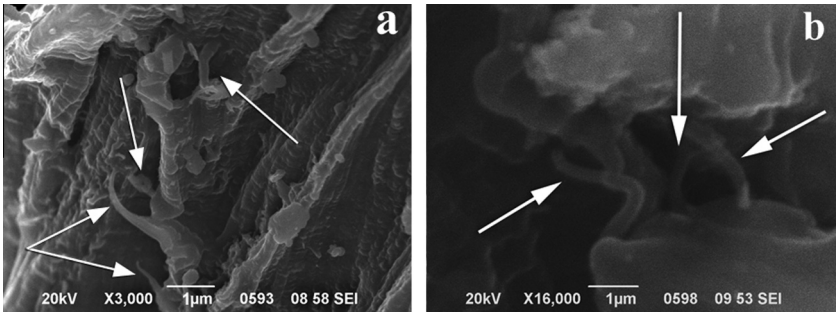

Fig. 12 – SEM image of the fracture surface after tensile testing of PEX nanocomposite containing 5% MWCNTs. The bridging MWCNTs interconnecting the polymer lumps are indicated by arrows.

Similar observations have been made for other polymer-CNTs nanocomposites reported in literature [16,48].

It is known that in a toughening process, after the application of stress, if the reinforcing tubes are not fractured they will bridge the polymer surfaces in the wake of a propagating crack and thus, they will hinder the crack opening [20]. From Fig. 12a and b this behavior is revealed as the tubes and bundles have fallen back onto the broken surfaces as a loosen network and they seem to be interconnecting the polymer lumps. The nanotubes and their bundles bridging across the cracks are indicated in Fig. 12a and b by arrows suggesting that stress release and absorption of the fracture energy is possible and therefore the fillers may result in a toughness improvement as suggested by the tensile testing results discussed in the previous sections. Also, some of the MWCNTs become loosened or curved, probably due to relaxation after fracture or uneven crack separation [16,48]. This interesting and typical breakage observation of the MWCNTs upon tensile stretching indicates a strong interfacial adhesion between MWCNTs and PEX matrix and a sufficient load transfer from the polymer to nanotubes. Similar observations have been made for other polymer matrices filled with MWCNTs [16,48].

Raman spectroscopy has been proved to be a useful tool for the examination of interactions between MWCNTs and polymer matrices and important theoretical and experimental work has been done concerning the Raman frequency shifts of the characteristic (G and D) bands of MWCNTs due to load transfer both in tension and compression [15,49]. Also many authors have combined the observed changes in the Raman spectra with the inter-tube interactions, disentanglement and dispersion of MWCNTs in polymer matrices [27,50,51]. Consequently, an investigation of the micro-Raman

spectra of the composites was essential for the better understanding of the reinforcement that MWCNTs cause in PEX.

In order to examine the possible load transfer between PEX and MWCNTs that was suggested by the measured tensile properties and SEM images, micro Raman measurements were performed in all the samples. In Fig. 13 the Raman spectra of PEX, MWCNTs and their nanocomposites are presented. Polyethylene's spectrum has been known for a long time and all the peaks of the spectrum of PEX can be assigned to the known PE bands [52]. The two main bands that appear in the spectrum of MWCNTs are most widely known as the G and D bands. The stretching of the C-C bond in graphitic materials gives rise to the "G-band" around 1600 cm^{-1} which is common to all sp^2 carbon systems, while the defects in the sp^2 carbon network activate an otherwise symmetry forbidden set of modes in the Raman spectrum leading to the first-order "D-band" around 1350 cm^{-1} [53].

It is obvious that the main peaks of polyethylene's spectrum can also be seen in the spectra of nanocomposites. From the spectra of the nanocomposites the presence of MWCNTs can also be seen from the G and D bands around 1600 and 1350 cm^{-1}, respectively. As the nanotubes' concentration increases, the polyethylene's peaks tend to decrease and eventually, as evidenced by similar composites in literature, the MWCNTs peaks dominate the spectra for filler loading higher than 10 wt% [50]. In Fig. 14 the considerable Raman peak up-shiftings for all the nanocomposites are shown compared to the peaks of MWCNTs. The peak positions of the G and D bands are 10–20 cm^{-1} up-shifted for all nanocomposites. Such an important difference has been found for other types of polyethylene when MWCNTs nanocomposites were studied [27,28,50,51,54,55]. The evident up-shifting has been attributed to the disentanglement of the MWCNTs bundles and their subsequent dispersion in the polymer matrix as well as to the strong compressive forces that the polymer matrix exerts on MWCNTs and successful load transfer between the fillers and the matrix [27,28,50,51,54,55]. In the present case of PEX nanocomposites the filler–matrix interactions were revealed from the obvious modifications of the shape

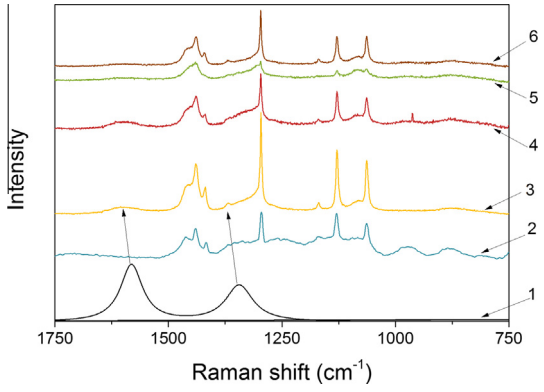

Fig. 13 – Raman spectra of (1) MWCNTs, (2) PEX and their nanocomposites containing (3) 0.5%, (4) 1%, (5) 3% and (6) 5% MWCNTs. (A colour version of this figure can be viewed online.)

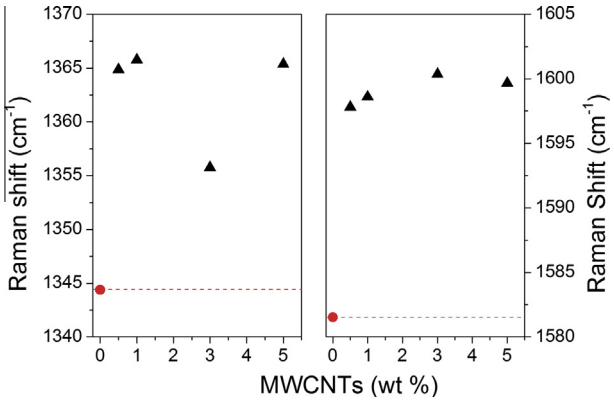

Fig. 14 – Raman peak shifts for the nanocomposites (squares) compared to the peak positions of MWCNTs (circles). (A colour version of this figure can be viewed online.)

and peak positions of the Raman spectra and the successful load transfer can be supported further with experimental evidence from microscopy observations and mechanical properties measurements.

4. Conclusions

In this work, novel nanocomposites of crosslinked high density polyethylene reinforced with MWCNTs were prepared and their mechanical properties were thoroughly examined. A significant improvement of mechanical properties was found for all nanocomposites. The combined results of tensile properties, SEM, TEM and Raman spectroscopy experimentally defined a major turning point for the elastic and deformation behavior in the composites, as for filler content below 1 wt% the composites retain the ductile behavior of the original polymer while higher loadings result in a more brittle performance. The detected turning point was successfully predicted from the micromechanical analysis using a unique combination of models corresponding to essentially the same concept but viewed in one case in its conventional form and in the other case in its more modern form. A three-phase model accounting for the matrix and two states of the filler, aggregated and dispersed, emerged from the micromechanical analysis for filler concentrations below 1 wt%, reflecting the necessity to adopt recent experimental findings in the mainstream micromechanical approaches. Above this concentration, the filler aggregates become larger and the original two-phase model can be considered more appropriate to interpret the experimental data. This behavioral change can be attributed to the participation of two competitive mechanisms governing the incorporation of MWCNTs in PEX: a tendency to enhance the mechanical properties of PEX by load transfer and a drive to form bundles that reduce the positive effect on these properties. Evidence of both these competitive mechanisms was found by micro-Raman spectroscopy and SEM observations of the failure surfaces. micro-Raman measurements suggested a successful load transfer between the matrix and the fillers while SEM observations revealed a fine dispersion at low

filler content and agglomerated nanotubes at higher filler concentrations.

Acknowledgement

This work was supported by the Greek General Secretariat of Research and Development (09SYN-33-484).

The authors would like to thank Prof. Aldo Boccaccini of the University of Erlangen-Nurnberg for allowing the use of the Raman spectroscopy facilities available at Biometerials Department and Mr. C. Dolle for performing these measurements. The authors would also like to thank Mr. N. Nianias, MSc, for his contribution in the nanocomposites preparation.

Appendix A. Supplementary data

Supplementary data associated with this article can be found, in the online version, at http://dx.doi.org/10.1016/j.carbon.2013.10.020.

REFERENCES

[1] Narkis M, Tzur A, Vaxman A, Fritz HG. Some properties of silane-grafted moisture-crosslinked polyethylene. Poly Eng Sci 1985;25(13):857–62.
[2] Ritums JE, Mattozzi A, Gedde UW, Hedenqvist MS, Bergman G, Palmlöf M. Mechanical properties of high-density polyethylene and crosslinked high-density polyethylene in crude oil and its components. J Polym Sci, Part B: Polym Phys 2006;44(4):641–8.
[3] Oliveira GL, Costa MF. Optimization of process conditions, characterization and mechanical properties of silane crosslinked high-density polyethylene. Mater Sci Eng, A 2010;527(18–19):4593–9.
[4] Dresselhaus MS, Dresselhaus G, Charlier JC, Hernández E. Electronic, thermal and mechanical properties of carbon nanotubes. Philos Trans R Soc London Ser A: Math Phys Eng Sci 1823;2004(362):2065–98.
[5] Ruoff RS, Lorents DC. Mechanical and thermal properties of carbon nanotubes. Carbon 1995;33(7):925–30.
[6] Kim P, Shi L, Majumdar A, McEuen PL. Thermal transport measurements of individual multiwalled nanotubes. Phys Rev Lett 2001;87(21):215502.
[7] Li HJ, Lu WG, Li JJ, Bai XD, Gu CZ. Multichannel ballistic transport in multiwall carbon nanotubes. Phys Rev Lett 2005;95(8):086601.
[8] Oberlin A, Endo M, Koyama T. Filamentous growth of carbon through benzene decomposition. J Cryst Growth 1976;32(3):335–49.
[9] Coleman JN, Khan U, Blau WJ, Gun'ko YK. Small but strong: a review of the mechanical properties of carbon nanotube–polymer composites. Carbon 2006;44(9):1624–52.
[10] Moniruzzaman M, Winey KI. Polymer nanocomposites containing carbon nanotubes. Macromolecules 2006;39(16):5194–205.
[11] Paul DR, Robeson LM. Polymer nanotechnology: nanocomposites. Polymer 2008;49(15):3187–204.
[12] Spitalsky Z, Tasis D, Papagelis K, Galiotis C. Carbon nanotube–polymer composites: chemistry, processing, mechanical and electrical properties. Prog Polym Sci 2010;35(3):357–401.
[13] Ajayan PM, Stephan O, Colliex C, Trauth D. Aligned carbon nanotube arrays formed by cutting a polymer resin-nanotube composite. Science 1994;265(5176):1212–4.
[14] Grossiord N, Loos J, Regev O, Koning CE. Toolbox for dispersing carbon nanotubes into polymers to get conductive nanocomposites. Chem Mater 2006;18(5):1089–99.
[15] Schadler LS, Giannaris SC, Ajayan PM. Load transfer in carbon nanotube epoxy composites. Appl Phys Lett 1998;73(26):3842–4.
[16] Ajayan PM, Schadler LS, Giannaris C, Rubio A. Single-walled carbon nanotube–polymer composites: strength and weakness. Adv Mater 2000;12(10):750–3.
[17] Loos MR, Schulte K. Is it worth the effort to reinforce polymers with carbon nanotubes? Macromol Theory Simul 2011;20(5):350–62.
[18] Chatterjee AP. A model for the elastic moduli of three-dimensional fiber networks and nanocomposites. J Appl Phys 2006;100(5):054302.
[19] Baxter SC, Robinson CT. Pseudo-percolation: critical volume fractions and mechanical percolation in polymer nanocomposites. Compos Sci Technol 2011;71(10):1273–9.
[20] Ward IM, Sweeney J. Mechanical properties of solid polymers. Wiley; 2012.
[21] Ouali N, Cavaille JY, Perez J. Elastic, viscoelastic and plastic behavior of multiphase polymer blends. Plast Rubber Compos Process Appl 1991;16(1):55–60.
[22] Halpin JC, Kardos JL. Moduli of crystalline polymers employing composite theory. J Appl Phys 1972;43(5):2235–41.
[23] Affdl JCH, Kardos JL. The Halpin-Tsai equations: a review. Polym Eng Sci 1976;16(5):344–52.
[24] Loos MR, Manas-Zloczower I. Micromechanical models for carbon nanotube and cellulose nanowhisker reinforced composites. Polym Eng Sci 2013;53(4):882–7.
[25] Uemura S, Takayanagi M. Application of the theory of elasticity and viscosity of two-phase systems to polymer blends. J Appl Polym Sci 1966;10(1):113–25.
[26] Campo N, Visco AM. Incorporation of carbon nanotubes into ultra high molecular weight polyethylene by high energy ball milling. Int J Polym Anal Charact 2010;15(7):438–49.
[27] Li S, Chen H, Cui D, Li J, Zhang Z, Wang Y, et al. Structure and properties of multi-walled carbon nanotubes/polyethylene nanocomposites synthesized by in situ polymerization with supported Cp_2ZrCl_2 catalyst. Polym Compos 2010;31(3):507–15.
[28] Ruan SL, Gao P, Yang XG, Yu TX. Toughening high performance ultrahigh molecular weight polyethylene using multiwalled carbon nanotubes. Polymer 2003;44(19):5643–54.
[29] Metın D, Tihminlioğlu F, Balköse D, Ülkü S. The effect of interfacial interactions on the mechanical properties of polypropylene/natural zeolite composites. Compos A Appl Sci Manuf 2004;35(1):23–32.
[30] Salvetat J-P, Briggs GAD, Bonard J-M, Bacsa RR, Kulik AJ, Stöckli T, et al. Elastic and shear moduli of single-walled carbon nanotube ropes. Phys Rev Lett 1999;82(5):944–7.
[31] Chabert E, Bornert M, Bourgeat-Lami E, Cavaillé JY, Dendievel R, Gauthier C, et al. Filler–filler interactions and viscoelastic behavior of polymer nanocomposites. Mater Sci Eng, A 2004;381(1–2):320–30.
[32] Favier V, Chanzy H, Cavaille JY. Polymer nanocomposites reinforced by cellulose whiskers. Macromolecules 1995;28(18):6365–7.
[33] Dagnon KL, Shanmuganathan K, Weder C, Rowan SJ. Water-triggered modulus changes of cellulose nanofiber nanocomposites with hydrophobic polymer matrices. Macromolecules 2012;45(11):4707–15.
[34] Capadona JR, Van Den Berg O, Capadona LA, Schroeter M, Rowan SJ, Tyler DJ, et al. A versatile approach for the

processing of polymer nanocomposites with self-assembled nanofibre templates. Nat Nanotechnol 2007;2(12):765–9.
[35] Bulota M, Jääskeläinen AS, Paltakari J, Hughes M. Properties of biocomposites: influence of preparation method, testing environment and a comparison with theoretical models. J Mater Sci 2011;46(10):3387–98.
[36] Stauffer D, Aharony A. Introduction to percolation theory. Taylor & Francis; 1994.
[37] Stauffer D, Bunde A. Introduction to percolation theory. Phys Today 1987;40(10):122–3.
[38] Balberg I, Anderson CH, Alexander S, Wagner N. Excluded volume and its relation to the onset of percolation. Phys Rev B 1984;30(7):3933–43.
[39] Celzard A, McRae E, Deleuze C, Dufort M, Furdin G, Marêché JF. Critical concentration in percolating systems containing a high-aspect-ratio filler. Phys Rev B 1996;53(10):6209–14.
[40] Azizi Samir MAS, Alloin F, Dufresne A. Review of recent research into cellulosic whiskers, their properties and their application in nanocomposite field. Biomacromolecules 2005;6(2):612–26.
[41] Pooyan P, Tannenbaum R, Garmestani H. Mechanical behavior of a cellulose-reinforced scaffold in vascular tissue engineering. J Mech Behav Biomed Mater 2012;7:50–9.
[42] Chen C, Baird DG. Dispersion of nano-clay at higher levels into polypropylene with carbon dioxide in the presence of maleated polypropylene. Polymer 2012;53(19):4178–86.
[43] Loos MR, Manas-Zloczower I. Reinforcement efficiency of carbon nanotubes – myth and reality. Macromol Theory Simul 2012;21(2):130–7.
[44] Ljungberg N, Bonini C, Bortolussi F, Boisson C, Heux L, Cavaillé JY. New nanocomposite materials reinforced with cellulose whiskers in atactic polypropylene: effect of surface and dispersion characteristics. Biomacromolecules 2005;6(5):2732–9.
[45] Dasari A, Duncan SJ, Misra RDK. Atomic force microscopy of plastically deformed polyethylene subjected to tensile deformation at varying strain rates. Mater Sci Technol 2002;18(6):685–90.
[46] Dasari A, Rohrmann J, Misra RDK. Microstructural evolution during tensile deformation of polypropylenes. Mater Sci Eng, A 2003;351(1–2):200–13.
[47] Ding W, Eitan A, Fisher FT, Chen X, Dikin DA, Andrews R, et al. Direct observation of polymer sheathing in carbon nanotube–polycarbonate composites. Nano Lett 2003;3(11):1593–7.
[48] Liu T, Phang IY, Shen L, Chow SY, Zhang W-D. Morphology and mechanical properties of multiwalled carbon nanotubes reinforced nylon-6 composites. Macromolecules 2004;37(19):7214–22.
[49] Hadjiev VG, Iliev MN, Arepalli S, Nikolaev P, Files BS. Raman scattering test of single-wall carbon nanotube composites. Appl Phys Lett 2001;78(21):3193–5.
[50] McNally T, Pötschke P, Halley P, Murphy M, Martin D, Bell SEJ, et al. Polyethylene multiwalled carbon nanotube composites. Polymer 2005;46(19):8222–32.
[51] Gorrasi G, Sarno M, Di Bartolomeo A, Sannino D, Ciambelli P, Vittoria V. Incorporation of carbon nanotubes into polyethylene by high energy ball milling: morphology and physical properties. J Polym Sci, Part B: Polym Phys 2007;45(5):597–606.
[52] Strobl GR, Hagedorn W. Raman spectroscopic method for determining the crystallinity of polyethylene. J Polym Sci: Poly Phys Ed 1978;16(7):1181–93.
[53] Dresselhaus MS, Jorio A, Hofmann M, Dresselhaus G, Saito R. Perspectives on carbon nanotubes and graphene Raman spectroscopy. Nano Lett 2010;10(3):751–8.
[54] Valentino O, Sarno M, Rainone NG, Nobile MR, Ciambelli P, Neitzert HC, et al. Influence of the polymer structure and nanotube concentration on the conductivity and rheological properties of polyethylene/CNT composites. Physica E 2008;40(7):2440–5.
[55] Jeon K, Lumata L, Tokumoto T, Steven E, Brooks J, Alamo RG. Low electrical conductivity threshold and crystalline morphology of single-walled carbon nanotubes – high density polyethylene nanocomposites characterized by SEM, Raman spectroscopy and AFM. Polymer 2007;48(16):4751–64.